

SEISMIC ANALYSIS OF RETAINING WALLS WITHIN PLASTICITY FRAMEWORK

T.Kalasin¹ and D. Muir Wood²

¹ Assistant Professor, Dept. of Civil Technology Education, King Mongkut's University of Technology Thonburi, Thailand.

² Professor, Dept. of Civil Engineering, University of Bristol, Bristol, UK
Email: t_kalasin@yahoo.co.uk, Thaveechai.kal@kmutt.ac.th

ABSTRACT :

Aseismic design of gravity wall still is a more difficult issue. The reason stems from the complexity of the problem which requires skills in soil mechanics, foundation engineering, soil-structure interaction along with knowledge of structure dynamics. Designing seismic gravity retaining structures deals with both kinematic interaction and inertial interaction but almost seismic building code neglected the soil-structure interaction by using the fixed base analysis of the structure. The gravity walls are a slender tall structure and it was suggested to be taken into account of dynamic soil-structure interaction analysis because such walls often perform badly when subjected to strong earthquake ground motion. Also the permanent displacement should be evaluated when designing the seismic gravity walls so that the need of the most reliable approach to evaluate a wall's vibration properties is required. In this paper, the alternative development of computed permanent responses was proposed in order to predict permanent responses of the seismic wall. The proposed model was constructed within the concept of macro-element modelling the soil, foundation and the seismic earth pressures. The constitutive law for modelling soil and foundation were based on two-surface kinematic hardening with associated flow rule. The development of seismic earth pressures was based on the Mononobe-Okabe method (1929) and the elastic-perfectly plastic method (Muir Wood and Kalasin(2004)) which based on the kinematic hardening by updating of a reference position for the wall. A parametric study is presented and The results are compared with published experimental results.

KEYWORDS: Earthquake, Gravity retaining wall, Earth Pressure.

1. INTRODUCTION

Gravity walls provide the lateral support for the higher side and must be protected from collapse to ensure the safety of building near the wall. The walls are most susceptible to earthquakes. Seismic damage to gravity wall results from foundation failure caused by excessive plastic ground deformation. Therefore the wall is unstable when the bearing capacity is declined whereas the wall tends to rotate and slide causing the wall damage. As the backfill exerts on the wall, it acts in the term of seismic inertia force on the wall. Thus the damage of a wall is mainly associated with the movement and failure induced by high seismic earth pressure. The seismic behaviour of retaining structures which uses its mass for stability against failure is considered an important design problem in seismic region. However, the available models in the literature were not completely achieved in order to predict the seismic response of the wall during earthquake. Not only the sliding mode is an important factor for designing gravity wall against earthquakes but also the tilting of rigid gravity wall is a majority of wall failure during earthquake. Although the determining the wall response was conducted by many researchers, the plastic displacement of the wall during earthquakes has been not emphasized for seismic design. This study is concerned with developing a macro-element model to analyze and understand the dynamic response of gravity wall to seismic excitation. The purpose of this research is to develop the implementation for predicting the seismic lateral earth pressure which is necessitated for design of earthquake resistant gravity wall. Generally, the stiffness of the wall, the backfill and the soil beneath the wall are required for investigating the interaction among them. The constitutive soil model for foundation is an important feature for predicting the coupled between the tilting and sliding of seismic retaining wall. The seismic lateral earth pressure needs to be modelled using reasonable the Mononobe-Okabe method and the interpolation of active and passive coefficient when the wall rotates and slides outward and forward. The proposed model is used in studying the dynamic response of gravity wall and also the parametric study is carried out to define the factors affecting the dynamic behaviour of the wall. The numerical results together with published experiments are discussed and used for evaluating the seismic response of gravity wall.

2. DYNAMIC LATERAL EARTH PRESSURES

Generally the Mononobe-Okabe formula was recommended by many researchers to evaluate the seismic lateral earth pressure but it was not available for the analysis case dealing with the time domain. Only the limited displacement approach based on the Newmark's block was appropriate for the mentioned problem. The wall performance was considered satisfactory by the limited displacement approach if the wall failed under sliding mode but not for the rocking mode. That is because the Newmark's method emphasized on the translational displacement and the aforementioned model predicts underestimating responses. As this study deals with the both elastic-plastic response of the wall during earthquake, the Mononobe-Okabe earth pressure formula was employed for evaluating the seismic lateral earth pressure. Also the fully passive and active forces thrust on the wall were established to incorporate with seismic movement. The assumption regarding by both sliding and rocking was carried out to investigate the matter response.

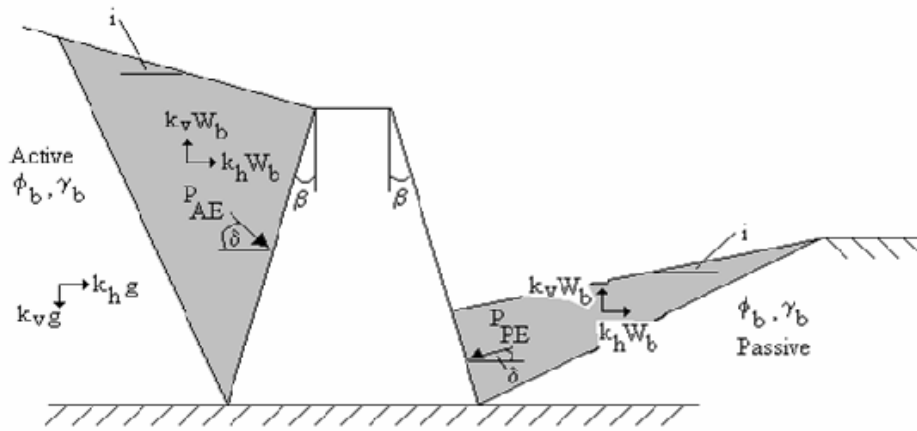


Figure 1 Schematic of seismic lateral earth pressures of the Mononobe-Okabe method(1929)

2.1. Mononobe-Okabe Earth Pressure

The dynamic lateral earth pressure on rigid retaining structures was developed in 1929 by Mononobe (1929) and Okabe (1926) who extended Coulomb's theory by including inertia forces.

$$P_{AE} = \frac{\gamma_b H^2}{2} (1 - k_v) K_{AE} \quad (2.1)$$

$$P_{PE} = \frac{\gamma_b H^2}{2} (1 - k_v) K_{PE} \quad (2.2)$$

$$K_{AE} = \frac{\cos^2(\phi_b - \varphi - \beta)}{\cos \varphi \cos^2 \beta \cos(\delta + \beta + \varphi) \left(1 + \sqrt{\frac{\sin(\phi_b + \delta) \sin(\phi_b - \varphi - i)}{\cos(\delta + \beta + \varphi) \cos(i - \beta)}} \right)^2}$$

$$K_{PE} = \frac{\cos^2(\phi_b - \varphi + \beta)}{\cos \varphi \cos^2 \beta \cos(\delta - \beta + \varphi) \left(1 - \sqrt{\frac{\sin(\phi_b + \delta) \sin(\phi_b - \varphi + i)}{\cos(\delta - \beta + \varphi) \cos(i - \beta)}} \right)^2}$$

Where γ_b is the backfill unit weight. H is the height of the wall. P_{AE} and P_{PE} are the dynamic active and passive earth pressures. K_{AE} and K_{PE} are the coefficient of dynamic active and passive earth pressures. ϕ_b is the internal friction angle of the backfill. i is the slope of the backfill with respect to the horizontal axis. δ is the friction angle between the inner face of the wall

and the backfill. β is the angle between the inner face of the wall and the vertical axis. k_h and k_v stand for the horizontal and vertical accelerations of the soil wedge in g unit so that $\varphi = \tan^{-1}(k_h/1 - k_v)$ but the wall is unstable when k_h is higher than $(1 - k_v)\tan\phi$. During earthquake, k_h and k_v are not constant and chaos so that, the seismic earth pressure in both active and passive cases are not constant. However, k_v is a great deal important but it usually assumed to be a half of horizontal acceleration or zero. Figure 2 illustrated the coefficient of seismic active and passive pressures when the wall induced with the various k_h and k_v when β and $\delta = 0$ and i is less than ϕ . The increase of vertical ground acceleration affected the increase of active and of passive earth pressure so that the degree of destructive of earthquake considered both horizontal and vertical acceleration is higher than that was assumed no vertical acceleration affected the wall. However the active and passive earth pressures only depended on the ground acceleration but also the translation and tilting of the wall. Thus the prediction of Mononobe-Okabe seismic earth pressure was collaborated with the elastic perfectly plastic model to enable the seismic active and passive earth pressure which depends on the wall movement.

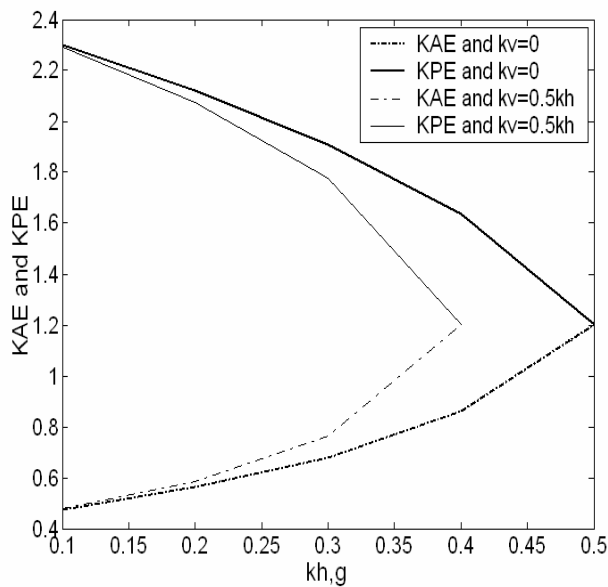


Fig 2. Seismic active and passive coefficient of earth pressure with various k_h and k_v

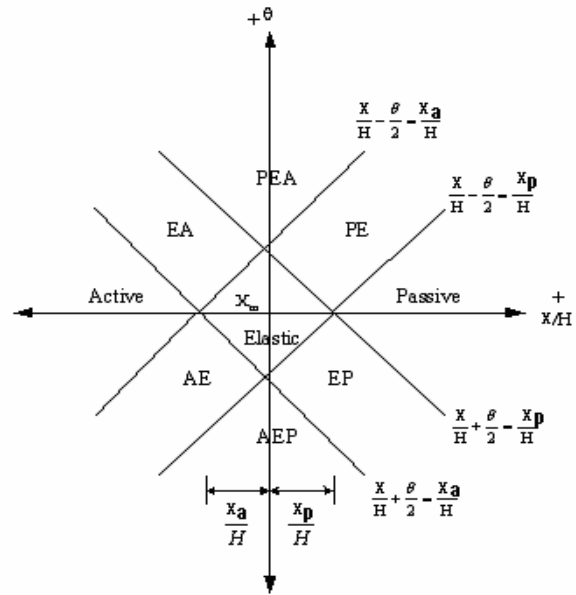


Fig 3. Regimes of response of rotating and translating wall of the perfectly plastic model. (Muir Wood and Kalasin (2004))

2.2. Elastic-Perfectly Plastic Model behind the wall

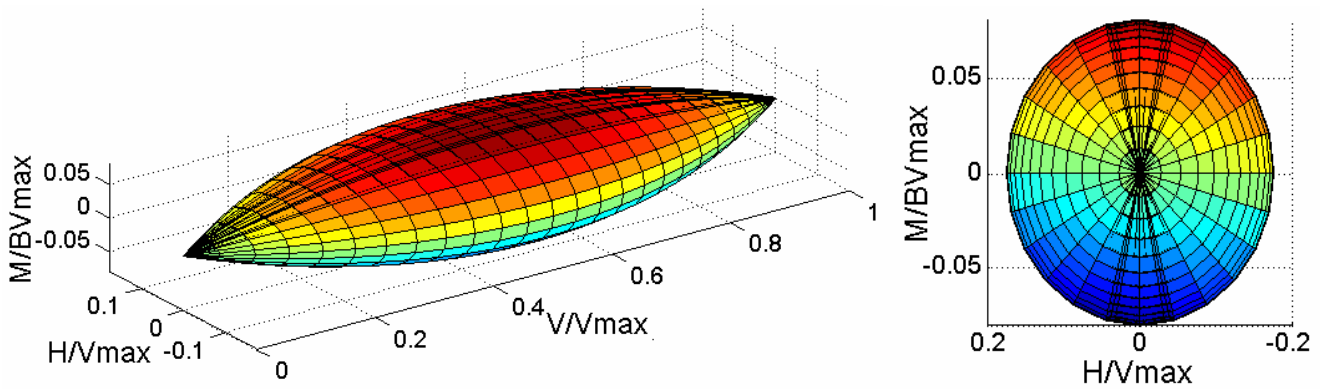
The development of the elastic-perfectly plastic model is based on the regime shown as Figure 3. The elastic regime needs to be added in the state of the wall regime. Limiting active and passive displacements are significant factors to identify the boundary of each regime. According to Table 1.1 proposed by Clough and Duncan (1991), the limiting active and passive displacements can be approximated and it is related with the backfill modulus, k_w which is also used to determine the elastic response of the wall be induced initially by the backfill and the earthquake motion. As the relationship of the coefficient earth pressure, the limited displacements and the soil modulus are used, the lateral earth pressure can be determined by using the nine different regimes of the wall in Figure 2 to compute the earth pressure regimes of elastic (E), passive (P), active (A), active-elastic (AE), passive-elastic (PE), elastic-active (EA), elastic-passive (EP), active-elastic-passive (AEP) and passive-elastic-active (PEA). (Muir Wood and Kalasin (2004)). So the force, F_w and moment, M_w acted behind the wall resulting from the earth pressure can be determined as Table 1.1. The suggested model for investigating the dynamic response of retaining wall assumed that the soil, the backfill materials and the foundation soil are dry dense sand and the wall is modelled as the rigid structure. The strength of soil material is modeled in the term of spring stiffness and their behaviour of both foundation and backfill is based on the constitutive model. This model consists of the failure surface together with an associated flow rule.

Table 1.1 Lateral Earth Pressure based on Mononobe-Okabe theory and Elastic-Perfectly Plastic Model

Mode	$\frac{F_w}{\frac{1}{6}\gamma_b H^2}$	$\frac{M_w}{\frac{1}{12}\gamma_b H^3}$
E	$3K_o + k_w(3(x - x_m) - \frac{\theta H}{2})$	$-\left(K_o + k_w((x - x_m) - \frac{\theta H}{2})\right)$
P	$3K_{PE}$	$-K_{PE}$
A	$3K_{AE}$	$-K_{AE}$
AE	$K(2 - \lambda_m - \lambda_m^2) + K_a(1 + \lambda_m + \lambda_m^2)$ where $\lambda_m = \frac{1}{2} + \frac{(x - x_a)}{\theta H}$ and $K = K_o + k_w((x - x_m) - \frac{\theta H}{2})$	$K(\lambda_m^3 - 1) - K_{AE}(\lambda_m^3)$
PE	$K_{PE}(1 + \lambda_m + \lambda_m^2) + K(2 - \lambda_m - \lambda_m^2)$ where $\lambda_m = \frac{1}{2} + \frac{(x - x_p)}{\theta H}$ and $K = K_o + k_w((x - x_m) - \frac{\theta H}{2})$	$-K_{PE}\lambda_m^3 + K(\lambda_m^3 - 1)$
EA	$K_{AE}(2 + 2\lambda_m - \lambda_m^2) + K(1 - \lambda_m)^2$ where $\lambda_m = \frac{1}{2} + \frac{(x_a - x)}{\theta H}$ and $K = K_o + k_w((x - x_m) + \frac{\theta H}{2})$	$K_{AE}(-1 - \lambda_m + 2\lambda_m^2 - \lambda_m^3) + K(1 - \lambda_m)^2\lambda_m$
EP	$K(1 - \lambda_m)^2 + K_{PE}(2\lambda_m - \lambda_m^2 + 2)$ where $\lambda_m = \frac{1}{2} + \frac{(x_p - x)}{\theta H}$ and $K = K_o + k_w((x - x_m) + \frac{\theta H}{2})$	$K(1 - \lambda_m)^2\lambda_m + K_{PE}(-1 - \lambda_m + 2\lambda_m^2 - \lambda_m^3)$
AEP	$K_{AE}(3\lambda_m^2 - 3\lambda_m\eta + \eta^2) + K_{PE}(-3\lambda_m^2 + 3\lambda_m\eta - \eta^2 + 3)$ where $\lambda_m = \frac{1}{2} + \frac{(x - x_a)}{\theta H}$ and $\eta = \frac{x_p - x_a}{\theta H}$ $\mathfrak{S}1 = \{3\lambda_m^2 - 3\lambda_m\eta + \eta^2 - 4\lambda_m^3 + 6\lambda_m^2\eta - 4\lambda_m\eta^2 + \eta^3\}$ $\mathfrak{S}2 = \{-1 - 3\lambda_m^2 + 3\lambda_m\eta - \eta^2 + 4\lambda_m^3 - 6\lambda_m^2\eta + 4\lambda_m\eta^2 - \eta^3\}$	$K_{AE}\mathfrak{S}1 + K_{PE}\mathfrak{S}2$
PEA	$K_{AE}(-3\lambda_m^2 - 3\lambda_m\eta - \eta^2 + 3) + K_{PE}(3\lambda_m^2 + 3\lambda_m\eta + \eta^2)$ where $\lambda_m = \frac{1}{2} + \frac{(x - x_p)}{\theta H}$ and $\eta = \frac{x_p - x_a}{\theta H}$ $\mathfrak{S}3 = \{3\lambda_m^2 + 3\lambda_m\eta + \eta^2 - 4\lambda_m^3 + 6\lambda_m^2\eta - 4\lambda_m\eta^2 - \eta^3\}$ $\mathfrak{S}4 = \{-1 - 3\lambda_m^2 + 3\lambda_m\eta - \eta^2 + 4\lambda_m^3 - 6\lambda_m^2\eta + 4\lambda_m\eta^2 + \eta^3\}$	$K_{PE}\mathfrak{S}3 + K_{AE}\mathfrak{S}4$

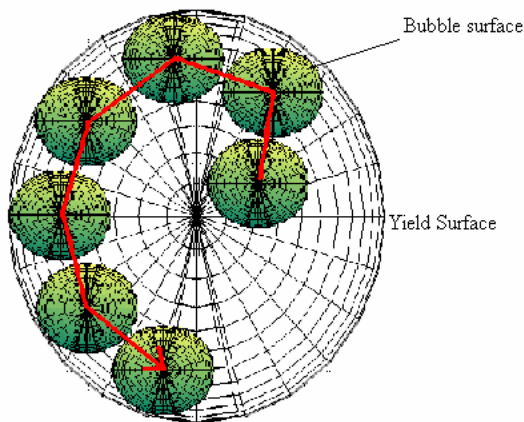
Now, the formulation of the wall macro-element is achieved. Ignoring the kinematic rule and varying the displacement and the rotation of the wall, the elastic-perfectly plastic wall model is illustrated in Figures 4a and 4b where $\phi_b = 25^\circ$ and $k_w = 65$ unit load/m. Wall height = 6m, $\gamma_b = 19.6$ kN/m³ and the horizontal acceleration, k_h varies from 0-0.4 g but the vertical acceleration, $k_v=0$ because k_v effects on only the magnitude of seismic pressures but not for the shape of the earth pressure model proposed herein. Most of retaining wall tends to collapse with the permanent displacement because the degrading of earth pressure depended on the wall velocity and movement in order to dissipate the driving energy. It is essential for modelling this behaviour aspect to valid the realistic model in time domain. The seismic force and moment thrust on the seismic wall based on the horizontal acceleration and collaborated with the kinematic rule illustrates in Figures 5a and 5b when $k_h = 0.4g$.

and Cremer (2001) for seismic loadings). Most of the wall moves initially in the elastic region but the behaviour of the wall on the sand moves with inelastic response. Therefore the boundary of the linear elastic region or the bubble was established for evaluating the stiffness (Al-Tabbaa, A. and Muir Wood, D (1989)). However it has the same shape but the size is different. This model was formulated in order to capture the elastic and inelastic response which occurs when the moment and horizontal loadings within the yield surface as shown in Figure 6a. The initial position of the bubble was based on the rest wall thrust by the backfill without unstable condition. The collapse wall under static condition was not taken in an account of this analysis. During unloading, the global behaviour of the foundation behaves purely elastically thus the uplift model was ignored thus the hardening law independent from the uplift behaviour of the foundation. The plasticity model comes from soil yielding under constant self weight of the wall. In this paper, the complete yield surface for combined loads reported by Butterfield and Gottardi (1994) was employed to determine the non-linearities at the sand-foundation interface. For a homogenous cohesiveless soil without tensile strength, the equation of the yield surface is shown in Figure 3 with the coefficients $\lambda_1 = \tan \phi_f$ and $\lambda_2 = 0.32$ for defining the size of the elliptic-yield surface in the plane between M/BV_{max} and H/V_{max} axes. V_{max} is foundation ultimate loading with friction angle at the ground surface. While the force and moment increase, the loading surface was dragged by horizontal and moment loadings. The loading path followed by the wall subjected to non-monotonic motions. The path starts from the wall in equilibrium state subjected to the gravity vertical loads and the lateral earth pressure at rest. So moment and horizontal loads are not equal to zero. ($M/BV_{max} \neq 0$ and $H/V_{max} \neq 0$). To simulate the kinematic translation of the ellipse translation whereas the loading is on the yield surface or the bubble surface, the two-surface proposed by Al-Tabbaa, A. and Muir Wood, D (1989) was used to describe the evaluation as equation (3.2).



a) 3D Yield surface where $\phi = 30^\circ$

b) Section of moment and horizontal loading of the yield surface



c) Translation of bubble surface where $V/V_{max} = 0.5$

Figure 6 The yield surface of footing on dense sand

$$\Gamma = \left(\frac{F_h}{\lambda_1} \right)^2 + \left(\frac{M}{B\lambda_2} \right)^2 - \left[V \left(1 - \frac{V}{V_{\max}} \right) \right]^2 \quad (3.1)$$

$$\Lambda = \left(\frac{F_h - \bar{\alpha}_h}{\lambda_1} \right)^2 + \left(\frac{M - \bar{\alpha}_m}{\lambda_2 B} \right)^2 - (rR_o)^2 = 0 \quad (3.2)$$

$$g = \left(\frac{F_h}{V_{\max} \kappa} \right)^2 + \left(\frac{M}{B V_{\max} \xi} \right)^2 + \left(\frac{V}{V_{\max}} \right)^2 - 1 \quad (3.3)$$

$$K_{ep} = K_e \left[I - \frac{\frac{\partial g}{\partial F} \frac{\partial \Lambda}{\partial F}^T K^e}{\frac{\partial \Lambda}{\partial F}^T K^e \frac{\partial g}{\partial F} + \Theta} \right] \quad (3.4)$$

Following the consistency rule, the kinematic hardening incremental vector, the plastic modulus (Θ based on translation of bubble surface and non-associated flow rule when $\Lambda = 0$) can be determined by considering the plastic potential surface as shown in equation (3.3) where $\kappa = 0.25$ and $\xi = 0.17$. The elasto-plastic stiffness can be computed as equation (3.4) when plastic multiplier is greater than 0. As the yield surface was not established to expand, the elasto-plastic stiffness K_{ep} was based on merely the associated flow rule when $\Gamma = \Lambda = 0$. The elasto-plastic stiffness was selected to substitute in term of foundation stiffness $[K_f]$ in equation (4.1) for evaluating dynamics response of the wall.

4. DYNAMICS EQUILIBRIUM AND COMPARISON BETWEEN MODEL PREDICTION AND EXPERIMENTS

The soil-wall system considered in the analysis is based on the dynamic equilibrium condition. The inertia forces acting on the wall, the resultant of the lateral earth pressure and the resultant of the bearing capacity of the soil-footing are considered. The inertia mass of the wall is considered and it is added in the term of mass matrix of the equation of the motion. The resultant of the bearing capacity was based on the limit equilibrium method and it was obtained in term of footing stiffness as described in section 3. Also the resultant of the lateral earth pressure is based on the proposed model as described in section 2. Therefore, the equation of horizontal motion can be formulated as:

$$[M]\{\ddot{x}\} + [C]\{\dot{x}\} + ([K_f] + [K_{wall}])\{x\} = \{-F_{ex}\} \quad (4.1)$$

where $[M]$ is the lump mass matrix of the wall including the inertia mass of the backfill and water pressure. $[C]$ is the viscous damping matrix computed by both the stiffness matrix of the wall-foundation, $[K_f]$ and the stiffness of the wall, $[K_{wall}]$. According to the behaviour of the wall, the lateral pressure at rest is not equal to zero therefore, the foundation should react in horizontal, vertical and rotational axes in order to maintain the wall in equilibrium. F_{ex} is external force matrix considering the ground acceleration and the earth pressure. Note that \ddot{x} , \dot{x} and x are the relative acceleration, velocity and displacement of the wall. Gazetas (1991) simplified the dynamic stiffness of the coupled horizontal and rocking vibrations. The coupled stiffness relationship was simplified to an uncoupled formulation assuming that the modulus of soil beneath the foundation increases with depth. The dynamic stiffness and damping of the strip foundation on the ground surface can be defined by equations (4.2) to (4.3) but the effect of free field motion is ignored.

$$K_{fx} = \frac{2}{2-\nu} G_o \left(1 + \frac{2}{3} \alpha \right)^n \quad (4.2)$$

$$K_{f\theta} = \frac{\pi}{2(1-\nu)} G_o B^2 \left(1 + \frac{1}{3} \alpha\right)^n \quad (4.3)$$

where B is the width of the wall. ρ_f is the density of the soil of the foundation. G_o stands for the shear modulus at the ground surface. K_{fx} and $K_{f\theta}$ are the static pure horizontal and rotational stiffnesses, respectively. The elastic stiffness of the backfill thrust on the wall is obtained by differentiate $\partial F_w / \partial x$ and $\partial M_w / \partial \theta$. In the case of dense sand, α and n are equal to 0 and 1 proposed by Gazetas (1991), respectively. The gravity retaining wall on Toyoura dense sands subjected to base shaking was performed by Okamura and Matsuo (2002) using the centrifuge test. The properties of the prototype wall and backfill are the width of the wall (B) = 4.5 m, the height of the wall (H) = 9 m, friction angle of soil footing (ϕ_f), friction angle of backfill (ϕ_b) = 41° and the relative density ($Dr\%$) = 82%. According to the experimental results generated by HongNam, Koseki and Sato (2007), the vertical young's modulus of Toyoura dense sands (E) = 338.3 MPa and shear modulus (G) = 117.8 MPa, poisson's ratio (ν) = 0.44697, initial void ratio (e_o) = 0.697, Ultimate vertical load of soil foundation (V_{max}) = 17.2 MN, Circular natural frequency of Toyoura sand (ω_n) is approximately 31 rad/sec and the damping ratio (ζ) = 5%. The wall was subjected to the sinusoidal motion containing amplitude = 0.4079g and frequency = 1.5 Hz.

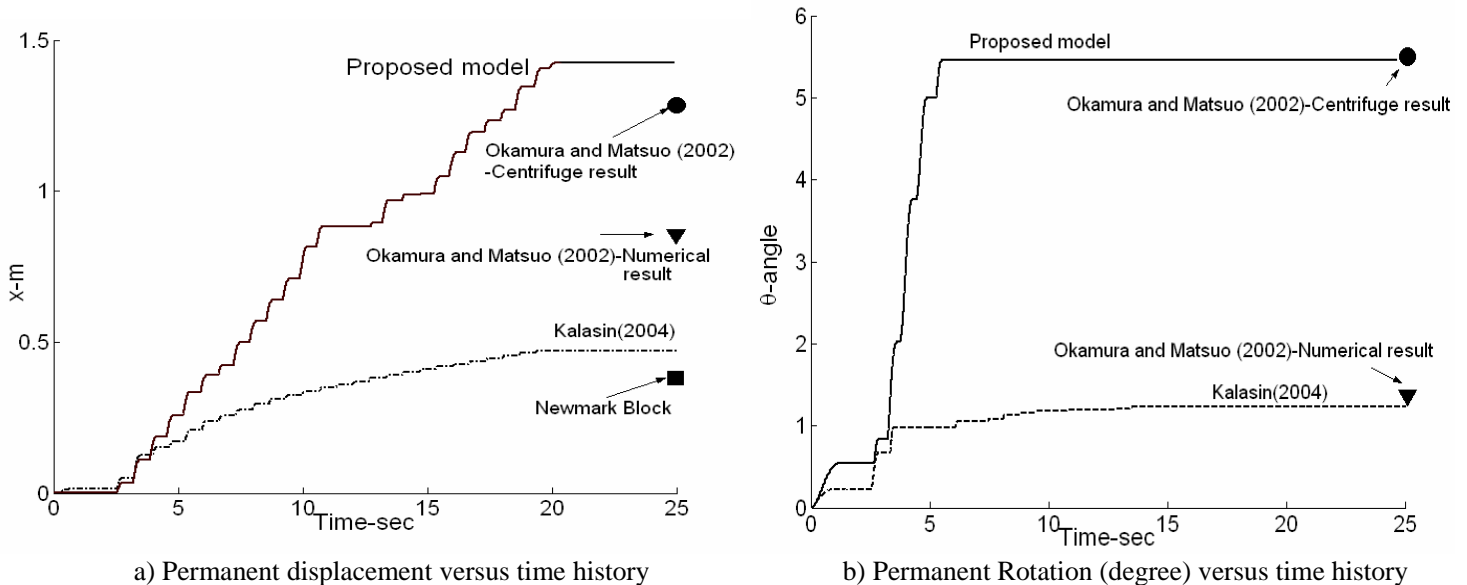
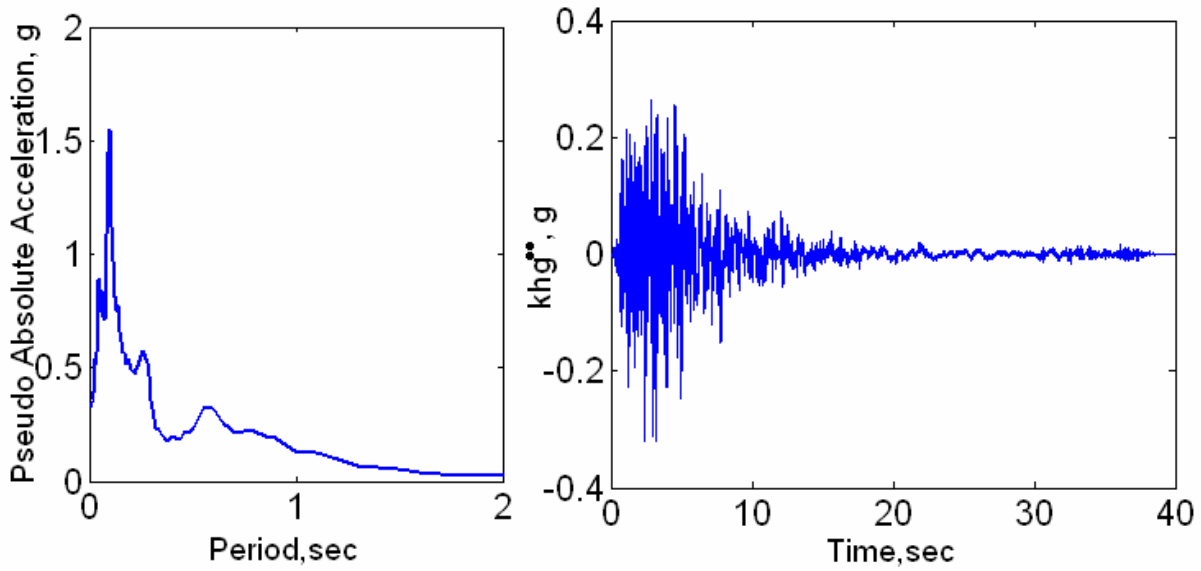


Figure 7. Observed and computed responses in prototype scale

The calculated response both horizontal displacement and rotation of the prototype wall subjected to sinusoidal wave is slightly greater than experimental results proposed by Okamura and Matsuo (2002) as shown in Figures 7a and 7b. The proposed method produced a reliable result. Main finding of the result shows that the updating the earth pressure based on the ground acceleration and the wall movement are essential to observe the seismic wall during earthquake by using the macro-element based on the constitutive frameworks. The systematic parametric study was conducted on a wall-soil system. One of features of the study relates to the soil nonlinearities during strong seismic excitation and the seismic lateral earth pressure thrust on the wall. The block wall is idealized of an actual wall. As this approach is available for time domain analyses, an excitation time histories of Chalfant Valley earthquake(1986/07/21 14:42), Station 54428 Zack Brothers Ranch having a peak horizontal ground acceleration about 0.4g shown in Figure 8a was used and the spectral acceleration of the earthquake illustrates in Figure 8b. The time integration method and the backward-Euler return mapping were employed to solve the response of the wall-soil system as illustrated in Figure 9. As this time history has a high frequency and amplitude, the wall was collapsed by the tilting mode during 1 to 10 seconds as shown in Figure 10. The pulse during 1 to 10 seconds and the peak acceleration at the third second causes the wall to lack of balance, so that the wall moves with progressive displacement and rotation.



a) Time history of Chalfant Valley Earthquake (PEER (2000)) b) Response spectra for 5% damping (PEER (2000))

Figure 8. Chalfant Valley (1986) motion and the response spectral acceleration

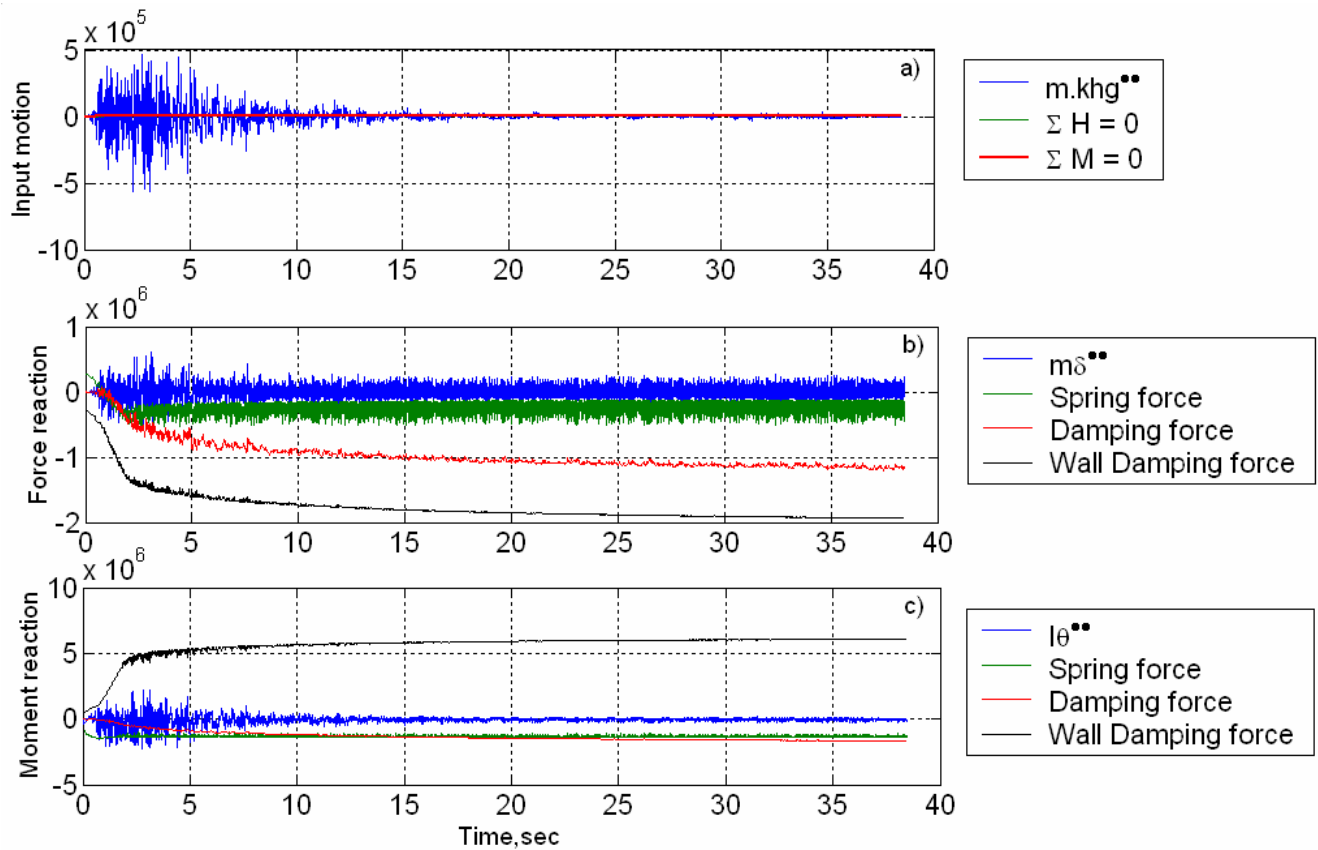


Figure 9. Responses of wall-soil system

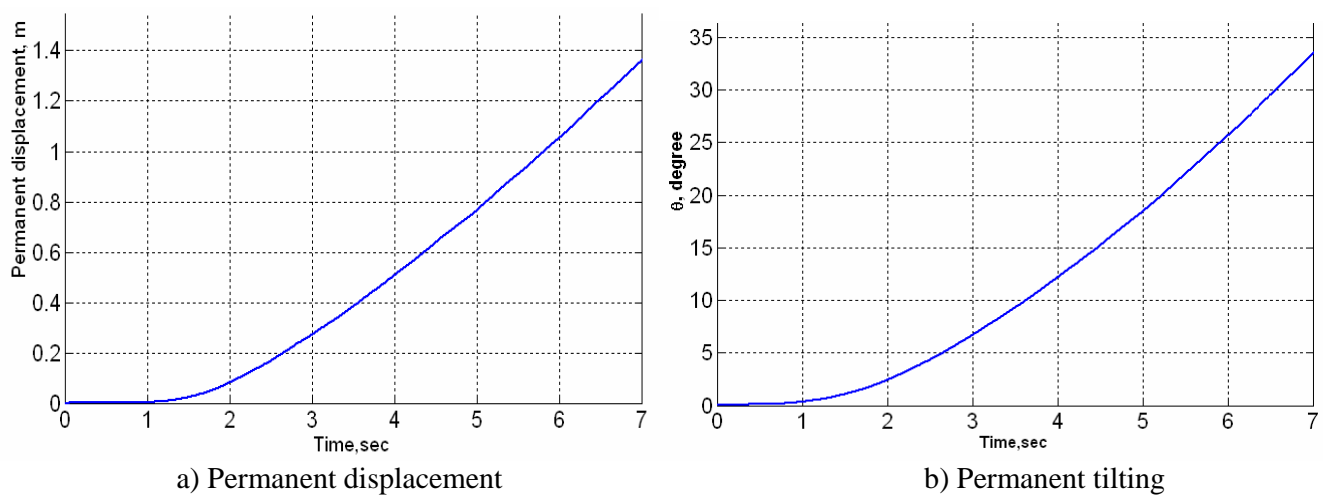


Figure 10 Permanent displacement and tilting angle of the wall subjected to Chalfant Valley Earthquake

Figure 10 illustrates that the wall moves outward from the backfill and the wall collapses with active regime at the end of ground acceleration. However, the wall might move from Active regime to AEP regime. This is because the wall moves toward to the backfill with the permanent tilting. In order to select the dimension of the wall which is able to resist the Chalfant Valley Earthquake, the wall movement affected by changing height and width of the wall lied on the Toyoura dense sands foundation, was investigated. The safe and unsafe zones were determined in order to select the width and the height of the wall. The increase of the width of the wall causes the wall to move in equilibrium state but it is not suitable when the economic reason was considered. In order to avoid the destructiveness resulted from the titling of the wall, the H/B ratio might be less than 1.78. Figure 11a illustrated that the wall begins to slide if the H/B ratio is higher than 1.44.

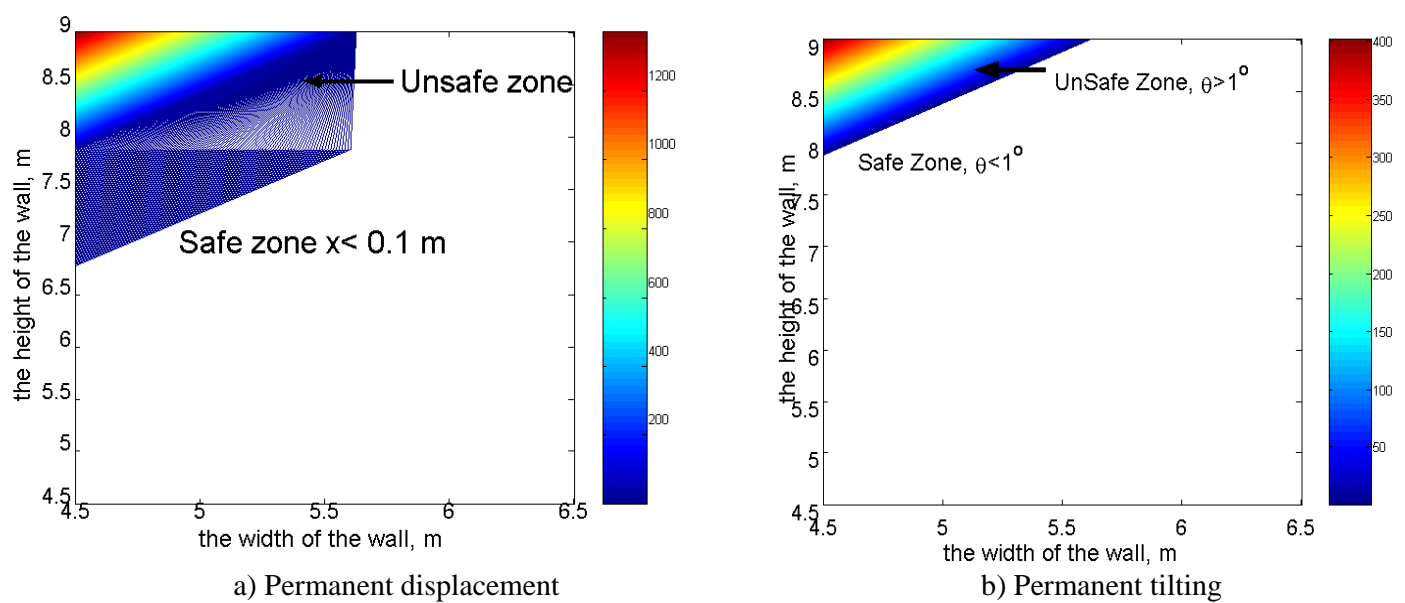


Figure 11 Safe and unsafe zones of the wall having different width and height subjected to Chalfant Valley Earthquake

6. CONCLUSION

A macro-element model was proposed to estimate the magnitude and the variation of the seismic earth pressures thrust acting on the back of the gravity wall induced with the ground acceleration. The proposed model was verified by comparing its result with the experiment result. As the Mononobe-Okabe approach is based on the pseudo-static and the magnitude of horizontal ground acceleration thrust on the back of the wall and the wall movement, have an important effect on the magnitude of seismic lateral earth pressures which is essential for designing the seismic wall. So the complexity of the dynamic interaction of the wall during earthquake can be solved by using the Elastic-Perfectly Plastic Model which is appropriate assumption for producing fully passive and active thrust. The constitutive model was a essential key for prediction of permanent displacement and rotation of the wall but the effective tool for experimental investigation to measure quasi-elastic properties such as Young's Modulus, shear modulus, poisson's ratio and damping ration should be considered. All of these reasons are strongly supported by centrifuge dynamic model test data proposed by Okamura and Matsuo (2002). The approach is appropriate for evaluating the response of the seismic wall which is useful when designing the wall in high risk earthquake zone.

REFERENCES

- Al-Tabbaa, A. and Muir Wood, D (1989). An experimentally based "Bubble" model for clay. *NUMOGIII*, Elsevier applied science: 91-99.
- Butterfield, R. and Gottardi, G (1994). A complete three-dimensional failure envelope for shallow footing on sand. *Geotechnique* **44:1**, 181-184.
- Clough, G. W. and Duncan, J. M. (1991). Earth pressure. *Foundation Engineering Handbook*. H.-Y. Fang. New York, Van Nostrand Reinhold: 223-235.
- Cremer, C. (2001) *Modelisation du comportement non lineaire des fondations superficielles sous seisme* PhD Thesis, Civil Engineering, LMT Cachan, ENS Cachan, France.
- Dafalias, Y. F. and Popov, E. P (1975). A model of nonlinearly hardening materials for complex loading. *Acta Mechanica* **21**, 173-192.
- Gazetas, G. (1991). Foundation vibration. *Foundation Engineering Handbook*. H.-Y. Fang. New York, Van Nostrand Reinhold: 553-593.
- Georgiadis, M. and Butterfield, R. (1988) Displacement of footings on sand under eccentric and inclined loads *Canadian Geotechnical Journal* **25**, 199-212.
- Goda, Y. and Abe, T. (1968). Apparent Coefficient of Partial Reflection of Finite Amplitude Waves, Port and Harbor Research Institute, Japan.
- Gottardi, G. and Butterfield, R. (1993) On the bearing capacity of surface footings on sand under general planar loads *Soil and Foundation* **33:3**, 68-79.
- HongNam, N., Koseki, J and Sato, T (2007). Effect of specimen size on quasi-elastic properties of Toyoura sand in hollow cylinder triaxial and torsional shear tests *Geotechnical Testing Journal* **31: 2**, 1-10.
- Kim, S. R., Kwon, O. S., et al. (2004). Evaluations of force components acting on gravity type quay wall during earthquakes *Soil dynamics and earthquake engineering* **24**, 853-866.
- Meyerhof, G. G. (1951). The bearing capacity of foundation under eccentric and inclined loads. *Proceedings of the 3rd International Conference on Soil Mechanics and Foundation Engineering*, Zurich: 440-445.
- Mononobe, N. (1929) *Earthquake Proof Construction of Masonry Dams* Proc. World Eng. Conf., **9**, 275.
- Muir Wood, D. and Kalasin, T. (2004). Macroelement for study of dynamic response of gravity retaining walls. *International Conference on "Cyclic Behaviour of Soils and Liquefaction Phenomena"*, Bochum, Germany, Taylor&Francis Group: 551-561.
- Nova, R. and Montrasio, L. (1991) Settlement of shallow foundations on sand *Geotechnique* **41:2**, 243-256.
- Okamura, M. and Matsuo, O (2002). A displacement prediction method for retaining walls under seismic loading. *Soil and Foundations* **42:1**, 131-138.
- Paolucci, R. (1997) Simplified evaluation of earthquake-induced permanent displacement of shallow foundations *Journal of Earthquake Engineering* **1:3**, 563-579.
- Pecker, A. (1997) *Analytical formulae for the seismic bearing capacity of shallow strip foundations* Seismic Behaviour of Ground and Geotechnical Structures, Balkema, Rotterdam, 261-268.
- PEER (2000). PEER Strong Motion Database. California, <http://peer.berkeley.edu/smcat/>, University of California.
- Salencon, J. and Pecker, A. (1995) Ultimate bearing capacity of shallow foundations under inclined and eccentric loads. Part I: pure cohesive soil *European Mechanics and Solid Journal* **14:3**, 349-375.